

Conference Paper

Improvement of Aortic Valve Stenosis Classification in Patients Through Computational Fluid Dynamics Model

Ioannis Makropoulos, Dimitris Zantzas, Vasilis Gkoutzamanis and Anestis Kalfas*

Aristotle University of Thessaloniki, Polytechnic School, Department of Mechanical Engineering, Thessaloniki, Greece.

* Corresponding Author Email: akalfas@auth.gr

ABSTRACT

Aortic valve stenosis (AS) is a common and severe valvular disease where accurate assessment is essential for determining prognosis and treatment. Current echocardiographic methods mostly rely on the simplified Bernoulli (SB) equation, which approximates the peak pressure drop (ΔP), risking poor stratification, especially for low-flow low gradient patients. This study examines the capabilities of combining computational fluid dynamics (CFD) and imaging techniques for better stratification of AS patients. Patient-specific geometries of the aortic valve, ascending aorta, and left ventricular outflow tract were reconstructed from CT and echocardiography data during peak systole. Inlet velocity boundary conditions based on ultrasound data enabled transient flow simulations. Blood flow was modeled as laminar and Newtonian, with the geometry discretized for computational efficiency without loss of accuracy. Validation against echocardiography data showed a 4% deviation in velocity predictions. Results indicated that ΔP and maximum velocity (V_{\max}) are strongly influenced by aortic valve area size, while leaflet geometry affects flow jet location. The CFD model revealed that SB overestimates ΔP in non-severe AS, potentially leading to misclassification. By combining CFD with precise imaging, detailed hemodynamic insights can be achieved, addressing the limitations of conventional methods and improving patient stratification for treatment.

Keywords—*Aortic valve stenosis, Patient-specific modeling, Stenosis categorization, Leaflet effects, Pressure drop, Maximum velocity, Hemodynamic flow field, Computational fluid dynamics.*

Copyright © 2024. This is an open-access article distributed under the terms of the Creative Commons Attribution License (CC BY): *Creative Commons - Attribution 4.0 International - CC BY 4.0*. The use, distribution or reproduction in other forums is permitted, provided the original author(s) and the copyright owner(s) are credited and that the original publication in this journal is cited, in accordance with accepted academic practice. No use, distribution or reproduction is permitted which does not comply with these terms.

INTRODUCTION

Cardiovascular diseases are the leading cause of death worldwide (32% in 2019)¹, and among them, aortic valve stenosis (AS) is one of the most serious. Initially, the aortic valve (AV) is one of the four valves of the heart, situated between the left ventricle (LV) and the ascending aorta (AA). This valve typically consists of three leaflets², which open and close during the cardiac cycle due to the pressure difference between the LV and AA, ensuring the unidirectional flow of blood towards the AA.

AS is typically attributed to the calcification of its leaflets, resulting in an increased workload on the LV. Specifically, due to the constriction of the cross-sectional area of the aortic valve area (AVA), the LV is required to generate higher pressure, thereby ensuring the appropriate pressure drop between the LV and the AA to maintain the flow of mass at normal levels. The primary method used for categorizing, *i.e.*, assessing, the severity of AS is the non-invasive echocardiography. The key parameters utilized in this measurement include the maximum measured velocity, calculated AVA and pressure drop.² Specifically, the pressure drop is estimated using the simplified Bernoulli equation (SB, $\Delta P_{SB} = 4 \times V_{vc}^2$ mmHg, where V_{vc} represents the velocity at the vena contracta, *i.e.*, the maximum velocity). Furthermore, it has been demonstrated that this equation tends to overestimate the actual pressure drop³, which could potentially impact patient assessment. The direct measurement of pressure drop can be achieved through invasive catheterization; however, this procedure carries inherent risks.

Accurate patient categorization is of vital importance, as from the moment AS symptoms appear, the annual survival rate decreases by 25%.⁴ Therefore, in recent years, there has been an increased demand for more effective assessment of individuals with AS and a deeper understanding of the flow field along the aortic valve. In this context, the goal of this research is to construct a computational fluid dynamics (CFD) model for simulating the flow along the aortic valve, utilizing real patient data. Additionally, another objective is to conduct a comprehensive analysis of the impact of aortic valve stenosis on the flow field. In this manner, this research aims to analyze the flow along the aortic valve for various constriction configurations,

thereby enhancing our understanding of the phenomenon and facilitating future investigations in the quest for an additional index that will serve as a supportive tool in patient categorization.

MATERIALS AND METHODS

Data from computed tomography (CT) and echocardiography (Echo) of a patient were acquired. From the CT data, the corresponding three-dimensional geometry was constructed for maximum diastole and systole using discretization software (Retomo, 2024, BETA CAE Systems International AG, D4 Business Village Luzern Platz 4, 6039 Root, Switzerland) (Figure 1 (a)→(b)). Subsequently, different software (ANSA, Beta) was used for processing and the improvement of the mesh (Figure 1 (b)→(c)). Additionally, the open AV's geometry was not discernible in the CT data at peak systole, likely due to the rapid nature of systole and the thinness of the leaflets. In contrast, the closed AV was distinguishable at maximum diastole. For this reason, the geometry of the open AV was constructed after processing the closed AV, and the geometric dimensions were validated using the echo data (Figure 1 (c)). Specifically, the AVA cross-section was nearly identical between the model and the echo (310 mm²). Subsequently, the enhanced geometries obtained at both maximum diastole and systole were integrated within the left ventricular outflow tract (LVOT) to facilitate the prescribed motion of the LV (Figure 1 (d)). However, it was found in the literature that this motion does not significantly affect pressure drop.⁵ Therefore, the prescribed left ventricle motion was chosen to be removed in order to reduce computational costs, and a conduit was placed in its position. Additionally, a second conduit was added to the ascending aorta to minimize the effect of boundary conditions on the results. The total dimensions of the two conduits are shown in Figure 1 (d), measured from the AVA.

To investigate the influence of AS and its valve leaflets on flow dynamics, a Python code was developed. This code, in conjunction with ANSA, facilitates the creation of various aortic valve geometries. Specifically, this code utilizes some basic geometric characteristics of the original valve and a user-defined percentage step. In this way, the desired AVA profiles are automatically generated in the

form of curves. Figure 2 depicts the geometries of the AV constructed with different AVA values.

The flow simulation was conducted using computational fluid dynamics software (ANSYS Fluent, R3, 2019). The simulation was time-varying (transient), and the valves in the fully open position during systole. The time step chosen was 10^{-3} seconds (it was found that variations between 10^{-3} seconds and 10^{-4} seconds result in a 0.03% deviation, while exponentially increasing computational cost). Incompressible fluid with a density of 1060 kg/m^3 and Newtonian fluid with a dynamic viscosity of $0.004 \text{ kg}\cdot\text{m/s}$ were considered. The boundary condition for the inlet referred to mass flow, for which it was assumed to follow a sin waveform, generating 90 ml (stroke volume, SV) during systole, which had a duration of 0.35 seconds (both values were derived from the echo data). The outlet boundary condition corresponded to a pressure, which was assumed to remain constant at 120 mmHg .⁶

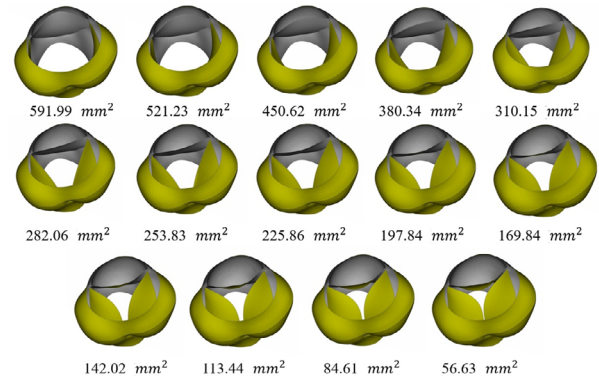


FIGURE 2. Different AVA cross-sections.

It was observed that the inflation layers introduced a deviation of 7.8% and 3.8% in ΔP and V_{\max} , respectively. For the investigation of the turbulence model, the low Reynolds SST model was chosen based on the literature.⁷ This model was used in conjunction with the volume mesh containing the inflation layers and produced $y_{\max}^+ (t) < 1.7 < 5$. Comparing the results between the laminar and turbulent flow models, differences of less than 0.8% were observed for both ΔP and V_{\max} . Therefore, the impact of the turbulence model appears to be minimal. Additionally, the accuracy provided by the introduction of inflation layers, relative to the additional computational cost, is considered negligible. For these reasons, and to reduce computational costs, the laminar flow model and the volume mesh without inflation layers were chosen. Additionally, before employing the two-volume meshes (one with inflation layers and one without), independent studies of the mesh were conducted. Specifically, for the volume mesh that was chosen for the simulations (without inflation layers), five different volume mesh sizes were examined: $0.4, 0.8, 1.6, 3, 9.6 \times 10^5$. Between the 4th and 5th volume meshes, there was a difference of 1.53% in ΔP and 0.98% in V_{\max} while between the 3rd and 4th volume meshes, the differences were 3.34% and 0.96% for ΔP and V_{\max} , respectively. The 4th volume mesh size was selected to reduce computational costs. The assumptions made regarding the mesh size, the choice of a volume mesh without inflation layers, and the use of laminar flow reduced the computational time for simulating the entire systolic cycle for one case from approximately 24 hours to 5 hours. The simulations were conducted on a laboratory computer with 32 GB RAM, a 512 GB SSD, and an 11th Gen Intel(R) Core™ i7-1165G7 processor.

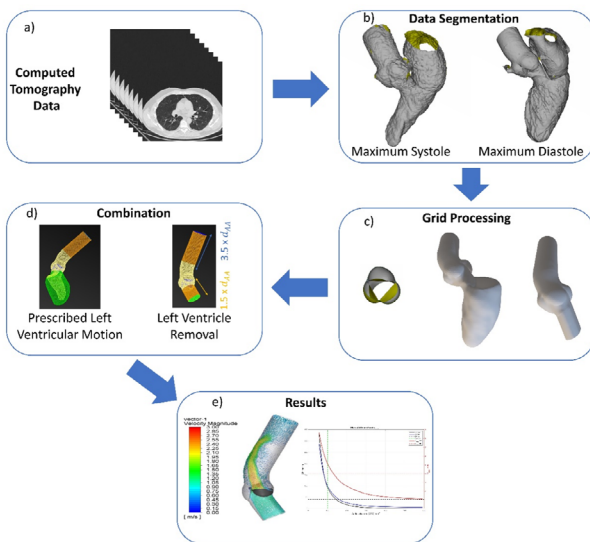


FIGURE 1. Representation of the methodology followed for the construction of the computational model. (d_{AA} diameter of the ascending aorta)

An investigation was conducted to assess the impact of inflation layers and turbulence model on the relevant parameters, pressure drop (ΔP), and maximum velocity (V_{\max}) at peak systole. The pressure drop was calculated based on the difference in static pressure between the level 45 mm before the AVA and 90 mm after the AVA.

RESULTS

For the validation of the model, initially, a comparison of the results with the measurements from the examined individual's echo was performed. The maximum velocity in the echo at the LVOT ranges from 1.13 to 1.22 m/s, while the corresponding velocity in the model is 1.27 m/s. Therefore, a 4% deviation in velocity is observed. Furthermore, at the peak of systole, the pressure drops and the maximum velocity calculated from the model are 2.79 mmHg and 1.63 m/s, respectively. Figure 3 presents the results of the AVA's impact on ΔP and V_{max} , as derived using the AV from Figure 2 and connected with spline curves. In the same diagram, the estimated pressure drop from SB is also depicted. The dashed lines indicate the thresholds for severe aortic stenosis condition.³

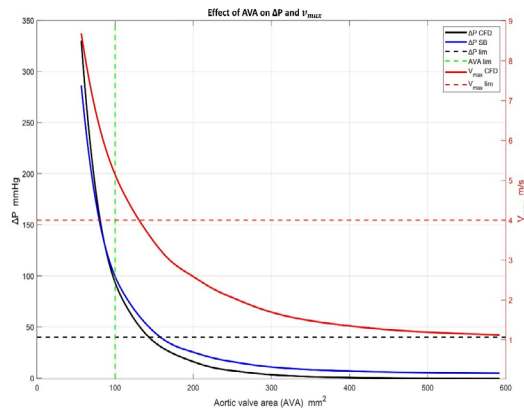


FIGURE 3. Effect of AVA cross-sections on flow characteristics.

To investigate the effect of each valve's geometry on the flow field, four different models with different AVAs were created (Figure 4). The first model represents the patient's initial AVA and serves as the baseline for comparison with the other three, which sequentially incorporate a dysfunctional valve. These dysfunctional valves were intentionally designed to achieve nearly identical AVA cross-sectional areas in all three cases. Simulation results showed that all three different aortic valves did not significantly differ in terms of the increase in ΔP and V_{max} . Specifically, the three dysfunctional AVs exhibited an average increase of +215% in ΔP and +125% in V_{max} .

Velocity Magnitude [m/s]
0.00 0.15 0.30 0.45 0.60 0.75 0.90 1.05 1.20 1.35 1.50 1.65 1.80 1.95 2.10 2.25 2.40 2.55 2.70 2.85 3.00

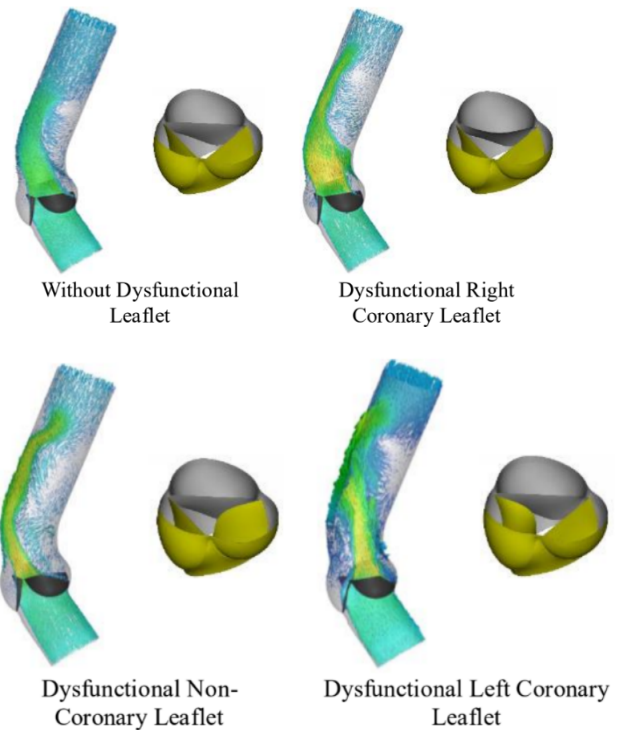


FIGURE 4. Models and flow patterns for assessing the impact of leaflets on the flow field.

DISCUSSION

The comparison made between the results and the echo data indicates that the model adequately predicts the flow field. Moreover, for a more comprehensive comparison, a comparison was conducted with patients from the literature^{5,8} who exhibited similar geometric and hemodynamic characteristics, including comparable AVA and stroke volume. From the comparison, deviations were observed, which can be attributed to the slight differences in these characteristics. For instance, V_{max} literature = 1.33 m/s, whereas V_{max} model = 1.63 m/s. The higher value in the model can be attributed to the smaller AVA and the greater maximum flow volume. Based on this analysis, the methodology utilized for constructing the three-dimensional model has demonstrated its effectiveness in calculating the maximum velocity and pressure drop at peak systole. In Figure 3, the high values of ΔP for severe AS are attributed to the constant stroke volume of 90 ml, whereas this volume is affected in cases of AS.

Therefore, the illustrated ΔP values correspond to the complete preservation of flow ($SV = \text{const}$) in the case of AS. Similar observations apply to V_{max} . Additionally, in the same figure, a pronounced overestimation of SB is observed in individuals with non-severe AS.³ Overall, based on the chart in Figure 3, clinical researchers could be able to assess the severity of stenosis in the specific patient for whom the model was created. Additionally, they could examine potential stenosis cases that may arise in the future.

Therefore, by applying the methodology presented for constructing the CFD model and valves, clinical researchers could create corresponding diagrams for each patient under examination. This would lead to a more comprehensive understanding of each examined individual by medical researchers. However, for this analysis to be applicable in clinical research, it is imperative to utilize supercomputers to minimize computational costs. Additionally, this methodology should be fully automated and thoroughly validated for accuracy across hundreds of patients. Based on the results obtained from the investigation of the leaflets, it was found that all three leaflets affect ΔP and V_{max} to a similar extent. Therefore, this leads to the additional conclusion that ΔP and V_{max} are not as strongly dependent on the geometry of the aortic valve as they are on the size of the AVA. However, the geometry of the AV affects the flow field, as depicted in Figure 4, where the flow jet location is different in the four cases. Hence, the valve's leaflets impact the location where the flow jet impinges on the AA, potentially contributing to the development of an aortic root aneurysm, as the impingement point in the ascending aorta can influence the Wall Shear Stresses.

CONCLUSION

In this research, a methodology was presented for constructing a patient-specific computational fluid dynamics model for simulating blood flow along the aortic valve. It was found that the model construction methodology is sufficient for calculating ΔP and V_{max} . Additionally, the code developed for automating the process of constructing various valves from the initial valve proved to be highly useful, as it can yield significant insights for future cases of more severe AS in the same patient. Furthermore, it

was revealed that in the patient's initial model, the inflation layers have a more pronounced effect on ΔP and V_{max} compared to the turbulence model, while the layers themselves are considered to provide negligible additional accuracy compared to the computational cost they introduced. Moreover, it was observed that all three leaflets exhibited a similar impact on ΔP and V_{max} , emphasizing that these parameters are predominantly influenced by the size of the AVA, rather than the specific valve geometry. However, the valve's geometry, specifically the leaflets, influences the flow pattern of the jet.

REFERENCES

1. World Health Organization, Cardiovascular diseases (CVDs). Available online: [https://www.who.int/news-room/fact-sheets/detail/cardiovascular-diseases-\(cvds\)](https://www.who.int/news-room/fact-sheets/detail/cardiovascular-diseases-(cvds)).
2. Ring, L., Shah, B.N., Bhattacharyya, S., et al. Echocardiographic assessment of aortic stenosis: a practical guideline from the British Society of Echocardiography. *Echo Res Practi*. 2021;8(1):G19–G59. <https://doi.org/10.1530/ERP-20-0035>.
3. Baumgartner, H., Stefenelli, T., Niederberger, J., et al. "Overestimation" of catheter gradients by Doppler ultrasound in patients with aortic stenosis: a predictable manifestation of pressure recovery. *J American Coll Cardiol*. 1999;33(6):1655–1661. [https://doi.org/10.1016/s0735-1097\(99\)00066-2](https://doi.org/10.1016/s0735-1097(99)00066-2).
4. Carabello, B.A. and Paulus, W.J. Aortic Stenosis. *Lancet*. 2009;373(9667):956–966. [https://doi.org/10.1016/S0140-6736\(09\)60211-7](https://doi.org/10.1016/S0140-6736(09)60211-7).
5. Hoeijmakers, M.J.M.M., Silva Soto, D.A., Waechter-Stehle, I., et al. Estimation of valvular resistance of segmented aortic valves using computational fluid dynamics. *J biomech*. 2019;94:49–58. <https://doi.org/10.1016/j.jbiomech.2019.07.010>.
6. Weese, J., Lungu, A., Peters, J., et al. CFD-and Bernoulli-based pressure drop estimates: a comparison using patient anatomies from heart and aortic valve segmentation of CT images. *Med Phys*. 2017;44(6):2281–2292. <https://doi.org/10.1002/mp.12203>.

7. Stewart, S.F.C., Paterson, E.G., Burgreen, G.W. et al. Assessment of CFD performance in simulations of an idealized medical device: results of FDA's first computational interlaboratory study. *Cardiovasc Eng Tech*. 2012;3:139–160. <https://doi.org/10.1007/s13239-012-0087-5>.
8. Yang, C.S., Marshall, E.S., Fanari, Z., et al. Discrepancies between direct catheter and echocardiography-based values in aortic stenosis. *Catheter Cardiovasc Interv*. 2016;87(3):488–97. <https://doi.org/10.1002/ccd.26033>.